Journal of Magnetism and Magnetic Materials 69 (1987) 53–60
North-Holland, Amsterdam

THERMAL AND MAGNETIC PROPERTIES OF $TbCl_3$

R. KREMER, E. GMELIN and A. SIMON

Max-Planck-Institut für Festkörperforschung, Heisenbergstr. 1, 7000 Stuttgart 80, Fed. Rep. Germany

Received 17 March 1987; in revised form 22 June 1987

The specific heat of polycrystalline $TbCl_3$ was measured in the temperature range $1.65\ K < T < 100\ K$. Magnetization and susceptibility of $TbCl_3$ were determined on polycrystalline and single crystal samples between $1.7\ K < T < 350\ K$. Our experimental data show ferromagnetic order of $TbCl_3$ below $T_c = (3.65 \pm 0.03)$ K. The magnetic entropy S_{mag} lost during ordering as calculated from the specific heat nearly corresponds to ln 2 indicating the ordering of a $S = \frac{1}{2}$ magnetic system. In the ordered state the magnetic moment orients along the crystallographic a-axis. The saturation moment is $(8.1 \pm 0.1)\mu_B$. The critical parameters $S_{mag}(T_c)$ and T_c/θ are determined and compared with theoretical calculations for 3D-Ising magnets. Our results are in best agreement with a previous neutron investigation performed by Murasik et al.

1. Introduction

The investigation of the thermal, magnetic and optical properties of rare-earth trichlorides has found particular interest in the past. Especially for the first half of the rare-earth series, the availability of large single crystals and their simple crystal structure stimulated a large number of experiments.

The trichlorides of the second half of the series are less well examined. In particular, there are only a few experimental investigations on $TbCl_3$, presumably because of difficulties based on crystallography: In the series of rare-earth trichlorides, $TbCl_3$ is the only one crystallizing at room temperature in the orthorhombic $PuBr_3$ structure (fig. 1) with space group Cmcm [1]. The situation with $TbCl_3$ is further complicated by the occurrence of phase transformations. Both the UCl_3-type [2] as well as the YCl_3-type structure [3] have been observed, leading to difficulties in the crystal growth from the melt [4].

The existence of rare-earth trihalide gas phase complexes with $AlCl_3$ offers a way of growing single crystals via chemical transport techniques [5,6]. This procedure yields single crystals of the low-temperature phase of $TbCl_3$ large enough for magnetization measurements.

The first neutron diffraction investigation of the magnetic properties of $TbCl_3$ powder was done by Murasik et al. [7]. They found long-range ferromagnetic ordering of $TbCl_3$ below 3.70 K. But from their powder data, they could not decide whether the magnetic moment is along the crystallographic a-axis (saturation moment $8.2(1)\mu_B$) or whether it is tilted about 20 degrees away from the a-axis into the a–b-plane (saturation moment $8.4(1)\mu_B$).

They propose a crystal field level scheme from inelastic neutron data giving an "accidental" doublet as the ground state. The doublet mainly contains $|J_z = \pm 6\rangle$ components of the $^7F_6$ ground

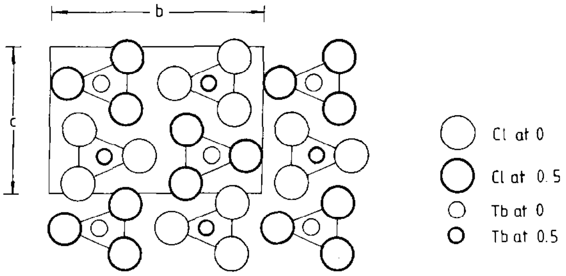

Fig. 1. Projection of the structure of $TbCl_3$ ($PuBr_3$-type) onto the b–c plane.

state multiplet. The first excited singlet lies approximately 6 meV $\approx k_B \times 70$ K above. Consequently $TbCl_3$ shows similar features as the hydroxyde $Tb(OH)_3$, although $Tb(OH)_3$ has the UCl_3-type crystal structure. $Tb(OH)_3$ orders ferromagnetically as well ($T_c = 3.72$ K [8–11]) and the properties of the ordered state can be understood by assuming an effective $S = \frac{1}{2}$ spin for the ground state and a highly anisotropic coupling of the Ising type between the moments. Two additional simple Tb salts are known that order ferromagnetically, $LiTbF_4$ at 2.86 K [12] and TbF_3 at 3.95 K [13,14].

The low ordering temperatures of the Tb salts indicate that very small exchange and dipolar forces contribute substantially to the magnetic interaction. In the past, terbium salts have, therefore, attracted much interest to study the effects of the long range dipolar forces on magnetic ordering [15–17].

2. Experimental

2.1. Sample preparation

Single crystals of $TbCl_3$ for our experiments were grown using a chemical transport technique [18]. Starting materials were Tb-oxide (purity 99.9%) from Rare Earth Prod. Ltd. and $AlCl_3$, which was prepared in situ by reacting aluminium with chlorine gas. The transport reaction was performed in a glass tube sealed under 1 atm of Cl_2 ($l \approx 20$ cm, temperature gradient $500\,^\circ C \rightarrow 400\,^\circ C$) [19]. Needle shaped $PuBr_3$-type single crystals ($l \approx 5$ mm, typically 2 mg) grew at the cold end of the tube. The needle axis was identified by means of X-rays to be the a-axis.

Powder samples of $TbCl_3$ were prepared from the Tb-oxide by reaction with NH_4Cl at 250 °C and purified by two distillations in tantalum crucibles under high vacuum [20].

The substance is hygroscopic, so all handling of the samples must be done in an inert gas atmosphere.

2.2. Specific heat measurements

Specific heats were measured in an adiabatic calorimeter designed for the examination of small samples [21]. Powders with typical masses of about 1 g were sealed in DURAN-glass ampoules under He gas to guarantee good heat contact.

The specific heats of the ampoules and the sample holder were measured separately and subtracted from the total measured heat capacity.

2.3. Magnetic entropy and magnetic internal energy

Magnetic entropy $S_{mag}(T)$ and magnetic internal energy $U_{mag}(T)$ were calculated by integrating $C_{mag}(T)/T$ and $C_{mag}(T)$, respectively following the thermodynamic relationships

$$S_{mag}(T) = \int_0^T C_{mag}(T')/T'\, dT', \tag{1}$$

$$U_{mag}(T) = \int_T^\infty C_{mag}(T')\, dT'. \tag{2}$$

The energy gap Δ_0 of an Ising system in the fully ordered state at $T = 0$ can be calculated from the magnetic internal energy $U_{mag}(0)$ by [22]

$$-U_{mag}(0)/R = \tfrac{1}{4}\Delta_0. \tag{3}$$

2.4. Magnetic susceptibility

The magnetization in the temperature range 1.7 K < T < 350 K was measured in a S.H.E. VTS susceptometer equipped with longitudinal and transverse pick-up facilities. The magnetometer was calibrated with $[(C_6H_5)_4As]_2Gd(NO_3)_5$ as a calibration standard assuming a magnetic moment of $7.9\mu_B$ per Gd^{3+} ion [23].

Single crystals of $TbCl_3$ were sealed in thin-walled quartz capillaries which were glued onto a Teflon sample holder so that the a-axis was parallel to the external field. Measurements of the transverse magnetization were performed by rotating the crystal around the a-axis and reading the projection of the transverse magnetization on the axis of the pick-up coil pair. Powder of $TbCl_3$ was pressed in cylindrical aluminium containers.

The magnetization of the sample holders and the containers were determined in a separate run and subtracted.

3. Experimental results

3.1. Specific heat

Our results of the total specific heat corrected for the calorimeter and ampoule contribution are shown in fig. 2b in a double logarithmic plot.

Below about 10 K, the onset of ferromagnetic order causes a λ-shaped anomaly. The Curie temperature, as estimated from the position of the C_p maximum, is $T_c = (3.65 \pm 0.03)$ K which is in good agreement with Murasik's value of (3.70 ± 0.05) K [7].

Above 10 K the lattice contribution as well as contributions from excited crystal field levels are dominant. Usually, for an estimate of the phonon contribution, C_{lat}, the specific heat of an isotypic nonmagnetic compound is measured. Such a compound was not available for the reasons cited in the introduction. Therefore, to obtain the pure magnetic contribution C_{mag} in the specific heat of $TbCl_3$, the following procedure was used: An effective temperature-dependent Debye temperature $\theta_D(T)$ was calculated by the Debye law from the total specific heat.

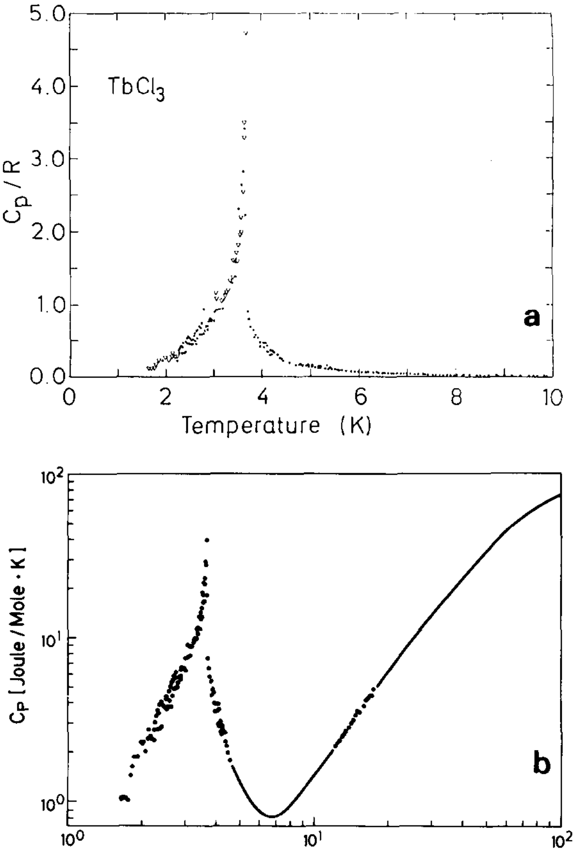

Fig. 2. (a) Magnetic part of the specific heat of $TbCl_3$ in the temperature range $1.65\ \mathrm{K} < T < 10\ \mathrm{K}$. Different symbols refer to two different samples; (b) the total heat capacity before subtracting the lattice contribution to the heat capacity. Solid lines are a guide for the eyes.

At about 10 K the value $\theta_D(10\ \mathrm{K}) \approx 178$ K was found. This value was used for lower temperatures in order to calculate the lattice contributions C_{lat} according to a power law [24]

$$C_{\mathrm{lat}}(T < 10\ \mathrm{K}) = 1944 \frac{\mathrm{J}}{\mathrm{mol\ K}} \left(\frac{T}{\theta_D(10\ \mathrm{K})} \right)^3 \qquad (4)$$

and then subtracted from the total specific heat to provide the magnetic part C_{mag} of the specific heat. This procedure partially covers the specific heat from the first excited crystal field singlet at approximately $\delta \approx 70$ K. The contribution of the excited state to the total specific heat is of the form $C_{\mathrm{sch}}/R = \frac{1}{2}(\delta/T)^2 \exp(-\delta/T)$ ("Schottky-tail") and in the order of 10% of C_{lat} at 10 K but exponentially decreasing for lower temperatures.

It we accept an uncertainty of about ±25 K for the Debye temperature below 10 K, the total errors arising from the above calculations should not exceed 3% for the magnetic entropy and 5% for the magnetic internal energy.

Hyperfine contributions C_{hyp} to the total specific heat (naturally occurring Tb is pure ^{159}Tb with $I = \frac{3}{2}$ giving rise to a hyperfine splitting) which were shown to be of the order of [15]

$$C_{\mathrm{hyp}}/R = (0.029 \pm 0.001) T^{-2} \qquad (5)$$

are negligible above 2 K and therefore are not taken into consideration when calculating C_{mag}.

Fig. 2a shows the magnetic part of the specific heat of two different powder samples of $TbCl_3$.

The magnetic entropy S_{mag}/R and the magnetic internal energy U_{mag}/R in the temperature range $1.65\ \mathrm{K} < T < 0\ \mathrm{K}$ are obtained by integration of $C_{\mathrm{mag}}(T)/RT$ and C_{mag}. For this purpose, the temperature axis was divided into three different sections. In the sections 1.65 K $< T < T_c$ and $T_c < T < 10$ K, the integration was done numerically after a careful smoothing of the experimental data. To evaluate the contribution to S_{mag}/R and U_{mag}/R for $T < 1.65$ K, the lowest experimentally reached temperature, we infer from fig. 2 that in the temperature range 1.65 K $< T < 3$ K the total specific heat can be very well approximated by a T^3-power law. The T^3-dependence was extrapolated down to 0 K and integrated analytically after subtracting the lattice part according to (4). The results, given in table 1, show that $S_{mag}(1.65\ \mathrm{K})/S_{mag}(\infty)$ is about 0.07 and $U_{mag}(1.65)/U_{mag}(0)$ about 0.03 so that we estimate the errors arising from this extrapolation for $S_{mag}(\infty)$ to be about 2% and for $U_{mag}(0)$ to be about 1%. Combining all contributions we finally found

$$S_{mag}(\infty)/R = 0.71 \pm 0.06 \tag{6}$$

which is in very good agreement with ln 2 = 0.693 for a magnetic system with effective spin $S = \frac{1}{2}$ and

$$-U_{mag}(0)/R = (2.3 \pm 0.1)\ \mathrm{K}. \tag{7}$$

Detailed information and a comparison with the experimental findings for $Tb(OH)_3$ is given in table 1. The temperature dependences of S_{mag}/R and U_{mag}/R are shown in fig. 3.

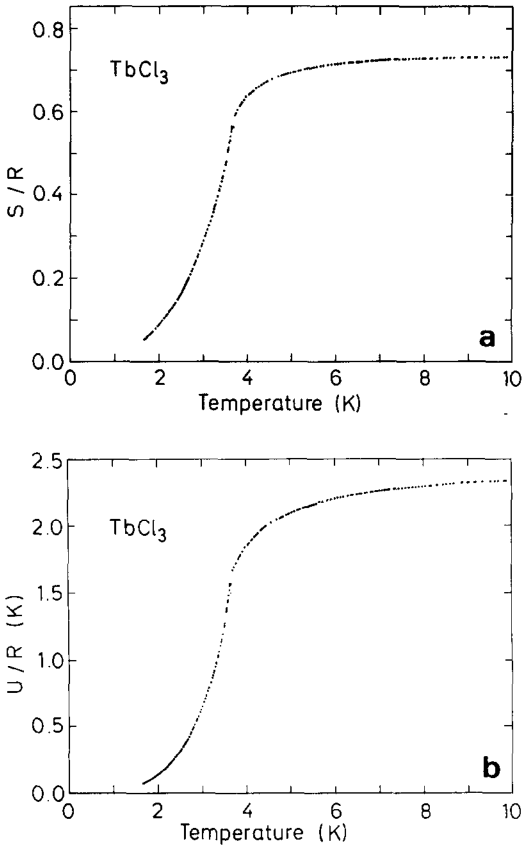

Fig. 3. (a) Magnetic entropy S_{mag}/R of $TbCl_3$ as obtained by numerically integrating $C_{mag}(T)/RT$; (b) magnetic internal energy temperature dependence.

3.2. Susceptibility and magnetization

The reciprocal molar susceptibilities of $TbCl_3$ powder and a single crystal (magnetic field parallel to the a-axis) is displayed as a function of temperature in fig. 4.

Analyzing the powder data at high temperatures, we observe that the magnetic moment is not constant but still slightly increasing and approaching the expected theoretical value of $9.72\mu_B$ for Tb^{3+} ions. At 350 K the effective magnetic moment μ_{eff} is

$$\mu_{eff}(350\ \mathrm{K}) = (9.6 \pm 0.1)\mu_B. \tag{8}$$

At low temperatures the susceptibility of the powder sample follows a Curie–Weiss law with a positive Curie–Weiss temperature indicating ferromagnetic ordering. The powder sample had the form of a small cylinder (6 mm $\varnothing$, $l \approx 5$ mm) so that uncertainties arise due to demagnetization effects when analyzing the low temperature data. Therefore, we limit the following discussion to the single crystal data.

The single crystal had the shape of a thin needle ($7 \times 0.4 \times 0.2$ mm^3; a-axis parallel to the needle axis). We calculated the demagnetization factor to be less than 0.6% using Osborne's formula [25]. Consequently a correction for the demagnetization was not carried out. At temperatures 4 K $\lesssim T \lesssim$ 60 K the reciprocal susceptibility rises linearly and can be analyzed using a simple Curie–Weiss law

$$\chi(T) = C/(T - \theta) \quad (4\ K < T < 60\ \mathrm{K}) \tag{6}$$

with the Curie–Weiss constant C and the

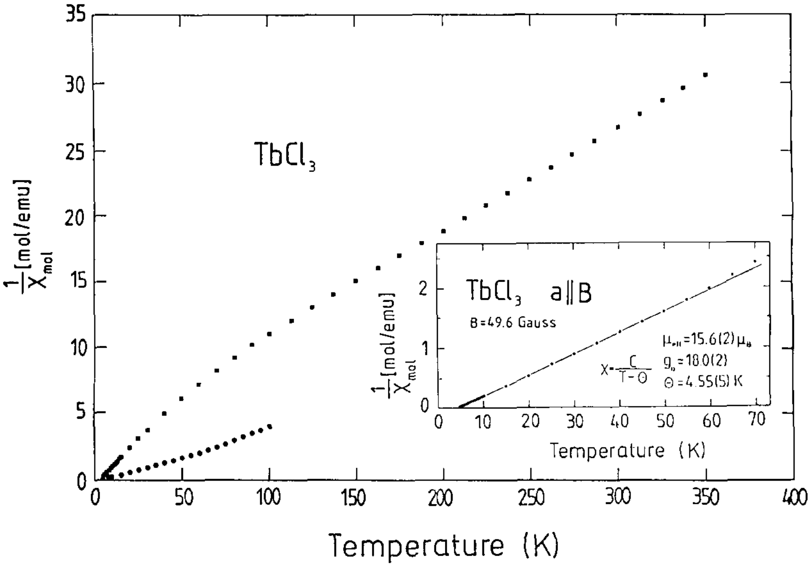

Fig. 4. (■) Reciprocal molar susceptibility of TbCl$_3$ powder, and (●) single crystal with magnetic field applied parallel to the crystallographic a-axis. The inset shows the experimental data of the single crystal on an enlarged scale.

Curie–Weiss temperature θ. Experimentally we found

$$C = (30.4 \pm 0.7) \text{ emu K/mol}, \tag{9}$$

$$\theta = (4.55 \pm 0.05) \text{ K}. \tag{10}$$

The parametrization of the crystal field given in Murasik et al. [7] enabled us to calculate the wave functions [26] of the crystal field levels and subsequently, the magnetic moment as a function of temperature.

Below 60 K, where the two lowest nearly degenerate singlets $|1\rangle$ and $|2\rangle$, $(E_2 - E_1 \approx 0.8$ K) are mainly populated, we found for the diagonal elements $\chi_{\alpha\alpha}(\alpha = x, y, z)$ using a formula given by Urland [27]

$$\chi_{zz} = N_L\, |\langle 1 | J_z | 2\rangle|^2 g_J^2 \mu_B^2 / k_B T \quad g_J = \tfrac{3}{2}, \tag{11a}$$

$$\chi_{xx} = \chi_{yy} = 0. \tag{11b}$$

A doublet with effective spin $S = \frac{1}{2}$ thus results in g-values of

$$g_z = 2g_J\, |\langle 1 | J_z | 2\rangle| \approx 17.3, \tag{12a}$$

$$g_x = g_y = 0. \tag{12b}$$

The result given in (12a) is in good agreement with the value observed experimentally.

Above 60 K, deviations from the Curie–Weiss law were seen indicating that excited crystal field levels are populated. It has been shown that striking deviations from a Curie–Weiss law appear roughly at a temperature of one third of the ground state isolation [28]. We infer from this that the next excited crystal field states contributing a magnetic moment, should be at approximately 180 K. This is in good agreement with Murasik's [7] findings that two singlets which can contribute a magnetic moment, are close together at 181 and 185 K.

The magnetization along the needle axis versus temperature in an external magnetic field of about 50 G is shown in fig. 5.

Below 4 K, the magnetization rises dramatically indicating the onset of long range ferromagnetic order. From the turning point of the magnetization curve, we determined the Curie temperature to be

$$T_c = (3.62 \pm 0.05) \text{ K}. \tag{13}$$

This is in very good agreement with the value found from the specific heat measurement.

At 1.7 K, our lowest experimental temperature,

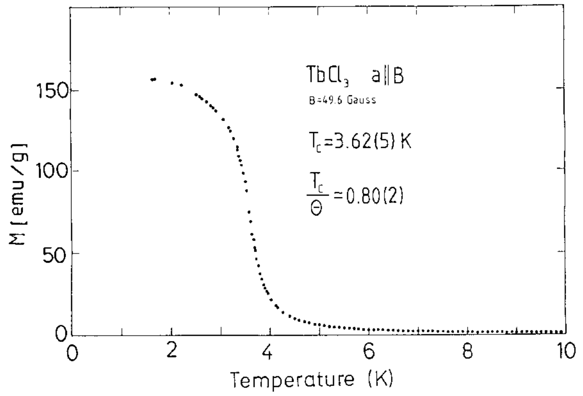

Fig. 5. Temperature dependence of the magnetization of a $TbCl_3$ single crystal with magnetic field applied parallel to the *a*-axis of the crystal.

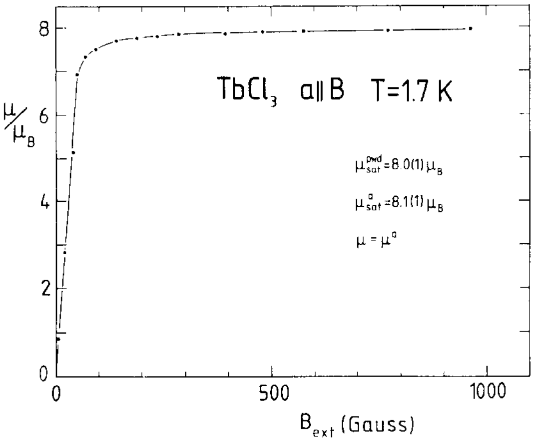

Fig. 6. Magnetization in units of μ_B of $TbCl_3$ at 1.7 K as a function of the applied external magnetic field.

the magnetization was nearly saturated. Its field dependence at 1.7 K is shown in fig. 6.

Saturation was already reached at magnetic fields of about 1 kG and the saturation moment per Tb^{3+} ion amounted to

$$\mu_{sat}^{a} = (8.1 \pm 0.1)\mu_B \qquad (14)$$

A similar experiment on a very fine powdered sample gave a saturation moment of

$$\mu_{sat}^{pwd} = (8.0 \pm 0.1)\mu_B \qquad (15)$$

in excellent agreement with the saturation moment along the *a*-axis of the single crystal. The powder was loosely filled into the aluminium container so that the crystallites could reorient in the external magnetic field (up to 5×10^5 G).

We measured the magnetization in the *b–c*-plane of a single crystal (as described above) to determine whether the magnetization was completely aligned along the crystal *a*-axis as suggested by the accordance of (14) and (15).

In our experiments we found that below 3.7 K the magnetization is less than 1 degree away from the *a*-direction. This small deviation might be due to an orientational error. Thus, we can conclude that Murasik's [7] second suggestion is correct, fixing the magnetization in the ferromagnetically ordered state exactly along the *a*-axis. In this case our saturation moment of $8.1(2)\mu_B$ is in best agreement with their finding of $8.2(1)\mu_B$.

4. Discussion of the critical parameters

In this section we want to give a brief discussion of the critical parameters of $TbCl_3$ listed in Table 1.

Following the analysis of the character of the exchange interaction in $Tb(OH)_3$ given by Catanese et al. [15], we expect similar conditions for $TbCl_3$. However, some difficulties might arise from the lower symmetry of the Tb site in $TbCl_3$ and from a small intermixing of a symmetric and antisymmetric combination of $|J_z = \pm 4\rangle$ components into the ground state wave functions [26]. From the close similarities between both compounds we conclude that the exchange interaction

Table 1
Thermodynamic quantities of $TbCl_3$ as derived from the specific heat compared with the results for $Tb(OH)_3$ [8–11,15]

	T_c (K)	$S_{mag}(\infty)/R$	$-U_{mag}(0)/R$ (K)	Δ_0 (K)	$S_{mag}(T_c)/R$
$TbCl_3$	(3.65 ± 0.03)	0.71 ± 0.06	(2.3 ± 0.01)	(9.2 ± 0.04)	0.56 ± 0.03
$Tb(OH)_3$	(3.72 ± 0.01)	0.68 ± 0.05	(2.3 ± 0.02)	(9.2 ± 0.08)	–

in $TbCl_3$ should be very well described by an anisotropic Ising Hamiltonian with spin $S=\frac{1}{2}$. For three-dimensional Ising systems ($S=\frac{1}{2}$) the critical entropy and energy parameters for lattices with different numbers of nearest magnetic neighbours have been published by several authors and are compiled, e.g. in ref. [29] (see references therein).

For $TbCl_3$ the critical parameters are

$$T_c/\theta = 0.80 \qquad (16)$$

and

$$S_{mag}(T_c)/S_{mag}(\infty) = 0.79. \qquad (17)$$

These values fit between those for a bcc and a fcc lattice of magnetic particles.

(bcc lattice: $T_c/\theta = 0.7942$; $S(T_c)/S(\infty) = 0.8396$; fcc lattice: $T_c/\theta = 0.8163$; $S(T_c)/S(\infty) = 0.8575$).

Fig. 7 shows the reduced magnetization M_a/M_0 of $TbCl_3$ plotted versus the reduced temperature compared with the spontaneous magnetization of a fcc $S=\frac{1}{2}$ Ising lattice as calculated by Guttmann et al. [30] and with molecular field predictions.

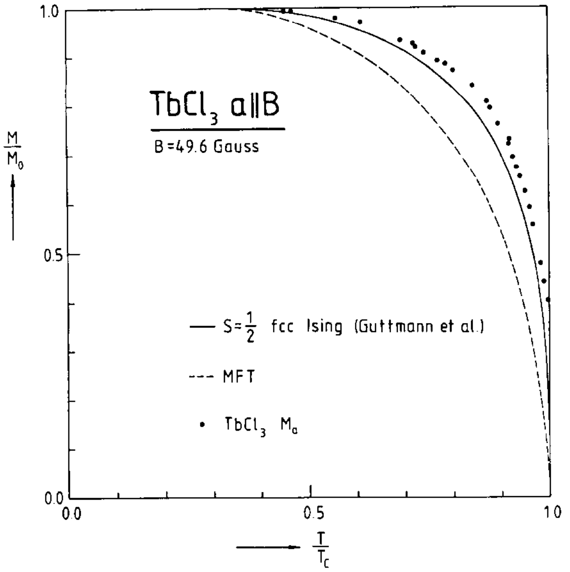

Fig. 7. Comparison of the magnetization ($B = 50$ G) of $TbCl_3$ with the spontaneous magnetization of a fcc Ising lattice for $S=\frac{1}{2}$ and the molecular field prediction.

These comparisons distinctly show that in $TbCl_3$ the number of magnetic nearest neighbours is high. So we can exclude a very anisotropic magnetic coupling between the moments on the Tb sites, as one might presume from the peculiarities of the crystal structure (see fig. 1) wherein the Tb atoms in the *a–c*-plane form layers which are loosely coupled along the *b*-direction.

5. Summary and conclusions

In this paper we report the thermal and magnetic properties of single crystals and powders of $TbCl_3$. To avoid difficulties from a polymorphic phase transition, single crystals for our experiment were grown in the $PuBr_3$-type structure by chemical transport. $TbCl_3$, like some other simple Tb salts, orders ferromagnetically. The magnetization lies along the crystallographic *a*-axis. Entropy considerations show that the ground state is best described by an effective $S=\frac{1}{2}$ spin.

In table 2 our experimental results are compiled. These results are in agreement with a previous neutron investigation of $TbCl_3$ powder by Murasik et al. [7]. From their crystal field analysis and the close analogy of the magnetic behaviour of $TbCl_3$ to $Tb(OH)_3$ found in our experiments, we are lead to the conclusion that the exchange interaction in $TbCl_3$ is of the Ising type.

A comparison of the critical parameters experimentally found with the results of model calculations for 3D-Ising systems shows that the "magnetic coordination" is high and somewhere in between a bcc and a fcc lattice, although the crystallographic structure suggests fewer magnetic neighbours.

From the crystallographic point of view $TbCl_3$

Table 2
Single-ion magnetic parameters for $TbCl_3$

Parameter	Value	Method
g_a	18.0(2)	Curie constant
	18.7(2)	sat. magnetization
μ_{sat}^{a}	8.1(1)μ_B	single crystal
μ_{sat}^{pwd}	8.0(1)μ_B	powder
θ	4.55(5)	low T susceptibility

is not as simple as $Tb(OH)_3$ and $LiTbF_4$, but further experiments might add to the knowledge of ferromagnetic ordering in insulators, especially the role of magnetic dipolar interactions in this context.

Acknowledgement

We thank Mr. M. Gehrke for the sample preparation and help with the susceptibility experiments and K. Ripka for technical assistance during the specific heat measurements.

References

[1] J.D. Forrester, A. Zalkin, D.H. Templeton and J.C. Wallmann, Inorg. Chem. 3 (1964) 185.

[2] Hj. Mattausch, A. Simon, N. Holzer and R. Eger, Z. Anorg. Allg. Chem. 466 (1980) 7.

[3] G. Garton and P.J. Walker, Mat. Res. Bull. 17 (1982) 1227.

[4] D.E. Fox and F.K. Fong, J. Cryst. Growth 20 (1973) 233.

[5] H. Schäfer, Chemical Transport Reactions (New York, London, 1964).

[6] H. Schäfer, Advan. Inorg. Chem. Radiochem. 26 (1983) 201.

[7] A. Murasik, P. Fischer, A. Furrer and W. Szczepaniak, J. Less-Common Metals 111 (1985) 177.

[8] W.P. Wolf, H. Meissner and C.A. Catanese, J. Appl. Phys. 39 (1968) 1134.

[9] P.D. Scott and W.P. Wolf, J. of Appl. Phys. 40 (1969) 1031.

[10] H.E. Meissner and W.P. Wolf, J. Appl. Phys. 49 (1969) 1038.

[11] A.T. Skjeltorp and W.P. Wolf, J. Appl. Phys. 42 (1971) 1487.

[12] L.M. Holmes, T. Johanson and H.J. Guggenheim, Solid State Commun. 12 (1973) 993.

[13] L.M. Holmes and H.J. Guggenheim, J. de Phys. 32 (1971) C1-501.

[14] L.M. Holmes, H.J. Guggenheim and G.W. Hull, Solid State Commun. 8 (1970) 2005.

[15] C.A. Catanese, A.T. Skjeltorp, H.E. Meissner and W.P. Wolf, Phys. Rev. B8 (1973) 4223.

[16] J. Als-Nielsen, L.M. Holmes and H.J. Guggenheim, Phys. Rev. Lett. 32 (1974) 610.

[17] J. Brinkmann, R. Courths and H.J. Guggenheim, Phys. Rev. Lett. 40 (1978) 1286.

[18] G.N. Papatheodorou and G.H. Kucera, Inorg. Chem. 18 (1979) 385.

[19] H. Gunsilius, R. Kremer and W. Urland, Z. Anorg. Allg. Chem., in print.

[20] A. Simon, N. Holzer and Hj. Mattausch, Z. Anorg. Allg. Chem. 456 (1979) 207.

[21] E. Gmelin and K. Ripka, Cryogenics 21 (1981) 177; W. Dai, E. Gmelin and K. Ripka, to be published in Cryogenics.

[22] M. Ball, M.J.M. Leask, W.P. Wolf and A.F.G. Wyatt, J. Appl. Phys. 34 (1963) 1104.

[23] R. Kremer and W. Urland, to be published.
W. Urland and R. Kremer, Inorg. Chem. 23 (1984) 1550.

[24] E.S. Gopal, Specific Heat at Low Temperatures (Plenum Press, New York, 1966).

[25] J.A. Osborne, Phys. Rev. 67 (1945) 351.

[26] We thank A. Furrer for providing us with the results of his calculations.

[27] W. Urland, Chem. Phys. Lett. 46 (1977) 457.

[28] G. Williams and L.L. Hirst, Phys. Rev. 185 (1969) 407.

[29] L.J. de Jongh and A.R. Miedema, Advan. Phys. 23 (1974) 1.

[30] A.J. Guttmann, C. Domb and P.F. Fox, J. Phys. 32 suppl. C-1 (1970) 354.